Chapter 3

Chloroplast Pigments: Structure, Function, Assembly and Characterization

Tatas Hardo Panintingjati Brotosudarmo, Leenawaty Limantara, Rosita Dwi Chandra and Heriyanto

Additional information is available at the end of the chapter

http://dx.doi.org/10.5772/intechopen.75672

Abstract

Chlorophyll and carotenoid are vital components that can be found in the intrinsic part of chloroplast. Their functions include light-harvesting, energy transfer, photochemical redox reaction, as well as photoprotection. These pigments are bound non-covalently to protein to make pigment-protein supercomplex. The exact number and stoichiometry of these pigments in higher plants are varied, but their compositions include chlorophyll (Chl) *a*, Chl *b*, lutein, neoxanthin, violaxanthin, zeaxanthin and β-carotene. This chapter provides introduction to the structure and photophysical properties of these pigments, how they assemble as pigment-protein complexes and how they do their functions. Various common methods for isolation, separation and identification of chlorophylls and carotenoid are also discussed.

Keywords: carotenoid, chlorophyll, core complex, ESI-MS/MS, high-performance liquid chromatography, light-harvesting antenna, photosystem, fluorescence spectrum

1. Introduction: Why do we bother about pigments in chloroplast?

Chlorophyll and carotenoid are important pigments that have been used as intrinsic optical molecular probes to observe plant performance during different phases of development. Chlorophyll and carotenoid are biosynthesized in chloroplast and their metabolism is closely related with the chloroplast development. Chlorophyll biosynthesis begins with the formation of 5-aminolevulinic acid (ALA) from glutamate (Glu) via Glu-tRNA synthetase, Glu-tRNA reductase (GluTR) and Glu-1-semialdehyde aminotransferase (GSA-AT) [1]. Eight molecules

IntechOpen

© 2018 The Author(s). Licensee IntechOpen. This chapter is distributed under the terms of the Creative Commons Attribution License (http://creativecommons.org/licenses/by/3.0), which permits unrestricted use, distribution, and reproduction in any medium, provided the original work is properly cited. CC BY

of ALA are condensed, eventually forming the symmetric metal-free porphyrin, protoporphyrin IX (Proto IX), which is a common precursor of haem and chlorophyll. The biosynthesis of chlorophyll continues by insertion of Mg^{2+} into Proto IX and followed by several steps in the chlorophyll cycle to create protochlorophyllide.

Further, reaction is one of the most interesting steps because this is the first step in chlorophyll biosynthesis that requires light: the NADPH:protochlorophyllide oxidoreductase converts protochlorophyllide into chlorophyllide. This reaction is then continued to produce chlorophyll (chl) *a* and *b*. So, when dark-grown etiolated seedlings are exposed to light, protochlorophyllide is immediately converted to chlorophyllide and then further to synthesis of chl. Once chl *a* and *b* are formed and properly incorporated into the thylakoid membranes and associated photosystems, chloroplast is fully functional to do photosynthesis [2].

Plant carotenoids are synthesized and accumulated exclusively in plastids, most importantly, chloroplast and chromoplast [3]. There are two types of plant carotenoid: carotene, which is cyclized and uncyclized hydrocarbons, and xanthophylls, which are oxygenated derivatives of carotenes. Carotenoid synthesis is initiated by the formation of C_{40} compound phytoene by the head-to-head condensation of two molecules of geranylgeranyl diphosphate (GGDP) by phytoene synthase and then to a series of 4 sequential desaturation reactions, by two separate enzymes to produce lycopene, which has 11 conjugated double bonds [4]. Lycopene is then cyclized to α-carotene or β-carotene, which is then further hydroxylated to produce colorful xanthophylls such as lutein, β-cryptoxanthin, zeaxanthin, antheraxanthin, violaxanthin and neoxanthin. The biosynthesis and accumulation of carotenoids in the dark-grown etiolated seedling are essential for the assembly of membrane structure and benefits the development of chloroplast when seedlings emerge into the light [5]. Understanding the relationship between structure and photophysical properties of these pigments can provide insights into a better study of how photosynthesis works at the molecular level in chloroplast.

2. Structure, function and photophysical properties

The photophysical properties and functions of chlorophyll and carotenoid reside in their chemical structure. Chlorophylls are defined as cyclic tetrapyrroles carrying a characteristic isocyclic five-membered ring that are functional in light-harvesting or in charge separation in photosynthesis [6]. The chemical structure with IUPAC numbering scheme of chl *a* is shown in **Figure 1**. It is a squarish planar molecule, about 10 Å on a side. An Mg atom in the center of the planar portion is coordinated to four nitrogen atoms. The five rings in chlorophylls are lettered A through E, and the substituent positions on the macrocycle are numbered clockwise, beginning in ring A. Chlorophyll has two molecular axes: *y*-axis is defined as passing through the N atoms of rings A and C and *x*-axis passing through the N atoms of rings B and D. The delocalized π electron system extends over most of the molecule, except for ring D, in which the C-17—C-18 double bond is reduced to a single bond. The tail is formed by condensation of four isoprene units and is then esterified to ring D. It is often called phytol tail, after the polyisoprenoid alcohol precursor that is attached during biosynthesis. Because of the reduced ring D, plant chlorophylls such as chl *a* and *b* are classified as chlorins rather than porphyrins. These types of pigments have (in organic solvents) absorption bands around the blue and red

http://dx.doi.org/10.5772/intechopen.75672

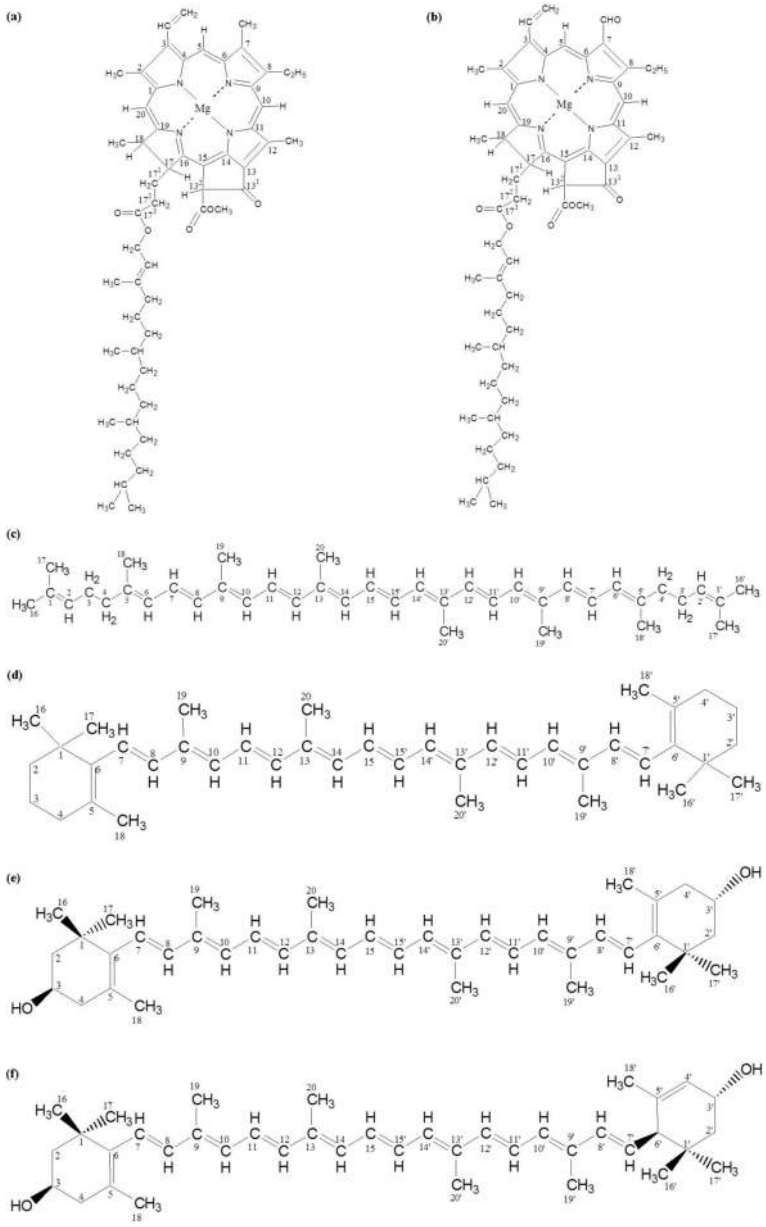

Figure 1. Chemical structure of Chl a (a), Chl b (b), lycopene (c), β-carotene (d), zeaxanthin (e) and lutein (f) with IUPAC numbering system.

spectral regions (**Figure 2a**), which are called B (or Soret) and Q bands, respectively, and arise from π→π* transition of the four frontier orbitals [7, 8]. One band each pair is polarized along the *x*-axis (B_x, Q_x) and other along *y*-axis (B_y, Q_y). The strong absorption band at the maximum

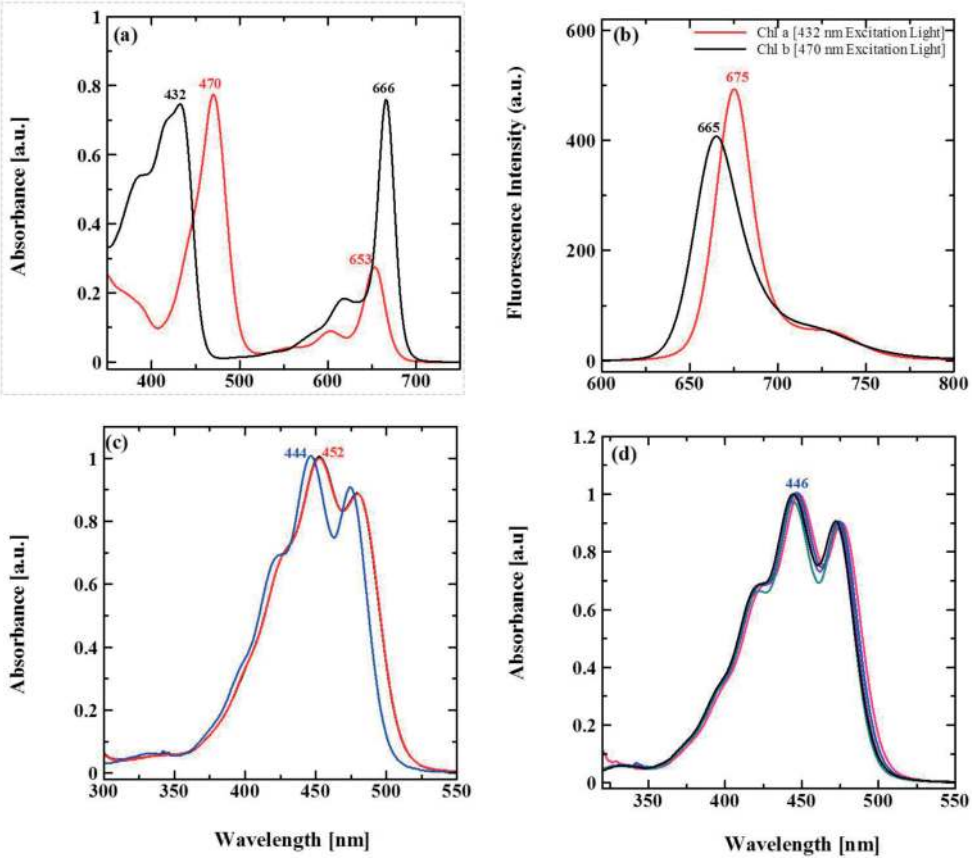

Figure 2. (a) UV–Vis absorption of Chl *a* (black) and Chl *b* (red) in MeOH, (b) fluorescence emission spectra of Chl *a* (red) and Chl *b* (black) in MeOH, (c) β-carotene (red), zeaxanthin (black) and lutein (blue) in EtOH, (d) lutein in several organic solvents; MeOH (black), acetone (pink), diethyl ether (purple), hexane (light blue), EtOH (blue).

absorption wavelength (λ_{max}) 660 nm is called Q_y transition band, which corresponds to the electronic transition polarized along the *y*-axis. The Q_x-band of chl *a* shows a weak band near 550 nm, while the two overlapping Soret (B) bands show at about 430 nm. The chemical structure of Chl *b* is identical to chl *a* except at the C-7 position, where a formyl group replaces the methyl group. This structural change results in a shift of the Q_y maximum absorption to shorter wavelength. The fluorescence spectrum of chlorophylls peaks at slightly longer wavelengths than the absorption maximum. The fluorescence emission (**Figure 2b**) is polarized along the *y* molecular axis, as it is emitted from the Q_y transition. Shift of the emission to the longer wavelength side of the main transition is known as Stokes shift. In light reaction, chlorophyll plays as key pigment in the collection of light energy in the light-harvesting complexes and to carry out reversible photochemical redox reaction (Krasnovsky reaction) in the reaction centers.

Structure of carotenoid is characterized by a linear chain of conjugated π-electron double bonds (**Figure 1**). In oxygenic organisms, carotenoid usually contains ring structures at each

end, and most carotenoids contain oxygen atoms, usually as part of hydroxyl or epoxide groups. The primary molecular factor that gives rise to their strong absorption bands in the visible spectral region is the number of π-electron conjugated double bonds, N. The position of the absorption maxima is affected by the length of the chromophore, the position of the end double bond in the chain or ring and the taking out of conjugation of one double bond in the ring or eliminating it through epoxidation. Progressive movement to longer wavelengths (bathochromic shift) is illustrated by the absorption spectra of the acyclic carotenoid of increasing chromophore length. Carotenoids show different optical characteristics in various solvents, depending on the polarizability of the solvent [9, 10]; however, generally they have a typical three-peaked absorption spectrum with well-defined maxima and minima (fine structure) (**Figure 2a**). A ring closure as in β-carotene produces a less-defined fine structure. The introduction of a carbonyl group in conjugation with the polyene system produces a bathochromic shift and the loss of fine structure [4]. The influence of other substituents such as OH is negligible, for example, β-carotene, cryptoxanthin and zeaxanthin all have very identical absorption spectrums. Owing to the double bonds in the molecule, all carotenoids exhibit *cis-trans* isomerization (stereomutation). A *cis* double bond implies a configuration with the highest-priority group on the same side, whereas in the *trans* configuration they are on opposite sides. The absorption spectrum of a *cis* isomer presents a subsidiary peak in the near-ultraviolet, the *cis* peak; generally, it is located 143 nm from the longest wavelength maximum. For example, *cis* peak will appear at 330 nm if the longest wavelength maximum is 473 nm. In photosynthetic systems, carotenoid has essential functions. First, carotenoid is an accessory pigment in the collection of light energy in the spectral region which chl does not absorb and in transferring energy to a chl pigment [11, 12]. Second, carotenoid functions in a process called photoprotection by quenching triplet state of chl before it reacts with oxygen to form singlet oxygen species (ROS) [13, 14]. Third, carotenoid regulates energy transfer in the light-harvesting antenna through a process called xanthophyll cycle, to avoid over-excitation of the photosynthetic system by safely dissipating excess energy [15, 16].

3. Pigment assembly in pigment protein complexes

In the chloroplast interior, there are four main constituents in plant thylakoids, that is, photosystem II (PSII), cytochrome b_6f, photosystem I (PSI) and the ATP synthesis. Chlorophylls and carotenoids are embedded in PS II and PSI, large pigment-protein clusters, the structures of which are perfectly adopted to ensure that almost every absorbed photon can be utilized to drive photochemistry. Both PSII and PSI consist of two moieties, that is, core complex or the reaction center that is responsible for charge separation and light-harvesting antenna complexes that surround the core complex and have functions to increase the capture of light energy and energy transfer to the reaction center in the core complex.

One can detect chlorophyll and carotenoid bound in PSII and PSI in chloroplast by measuring their absorption and fluorescence spectra. **Figure 3a** (solid red line) shows the absorption spectrum of diluted chloroplast that is indicated by red shift of Chl *a*, Chl *b* and carotenoid's bands because these molecules are bound as pigment-protein complexes in chloroplast. The Soret band of chl *a* in the complexes was detected at 438 nm while in the MeOH it was found

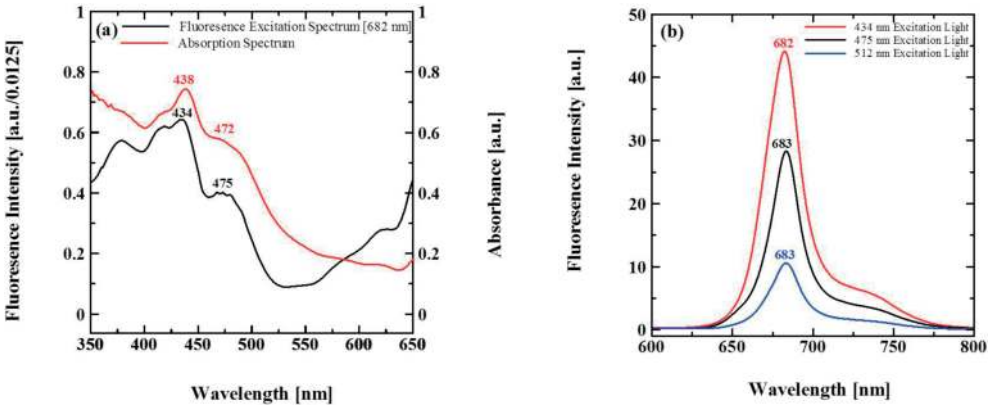

Figure 3. (a) Overlaid of UV–Vis absorption (red) and fluorescence excitation (black) (λ_{em} = 682 nm) spectra of chloroplast and (b) emission spectra of chloroplast with excitation at 434 (black), 475 (red) and 512 (blue) nm. Measurements were conducted at ambient temperature. The isolation of chloroplast was carried out as follows: 20 g of suji leaves (*Pleomele angustifolia*) were washed with running water and cut. The leaves were then homogenized in 200 mL ice-cold isolation buffer (300 mM sorbitol, 50 mM HEPES-KOH pH 7.5, 2 mM EDTA, 80% acetone, 0.1% BSA) for 10 min in a cold environment, followed by filtration using cloth. Centrifugation was conducted in 2 steps, to discard cell debris at 200 g, 4°C, 20 min and to harvest chloroplast pellet at 3000 g, 4°C, 20 min. Final chloroplast pellet was collected and subjected to spectrum UV–VIS (Shimadzu UV-1700)and fluorescence measurement (Jasco FP-8500).

at 432 nm (**Figure 2a** black line). The fluorescence emission spectra (**Figure 3b**) indicate a strong emission band of PSII complexes with maximum wavelength at (λ_{max}) about 682 nm and weak emission band of PSI complexes with λ_{max} at about 730 nm. It is shown here that Chl *a* acts as the main contributor to the excitation band at 434 nm and it shows that excitation at 434 nm (Soret band) produces stronger emission intensity, while the excitation at 475 and 512 nm, correspond to Chl *b* Soret band and carotenoid, respectively, produces weaker emission intensity. If we monitor the emission at 682 nm and measure the excitation spectrum, it shows that the PSII emission at 682 nm is the result of contribution from Chl *a*, Chl *b* and carotenoids (**Figure 3a** solid black lines) with bands at λ_{max} about 414, 434, 475 nm, respectively.

The current high-resolution structural models of antenna complexes have been obtained only for LHCII (2.72 Å) and recently for CP29 (2.8 Å) from PSII of spinach [17, 18]. Here we focus more on the LHCII structure. LHCII shows trimeric structure. Each monomeric contains three transmembrane α-helices, a, b and c (**Figure 4a**). One monomeric subunit contains eight chlorophyll (Chl) *a* pigments, six Chl *b*, two luteins (Lut), neoxanthin and one additional xanthophyll [17, 19]. The 14 chlorophylls are non-covalently attached in the protein cavity. Four carotenoid binding sites per monomer have also been characterized, but in this case the type of carotenoid bound can vary. Typically, two lutein molecules are in groves on both sides of helices *a* and *b* and have been likened to a cross-brace. A third carotenoid, 9-*cis* neoxanthin, is located in the Chl *b*-rich region near helix *c*. The fourth carotenoid is located at monomer-monomer interfaces in the trimer. It has been suggested that this site accommodates carotenoids that can participate in the xanthophyll cycle. It depends on the external stress level of the plant; the fourth carotenoid is either violaxanthin (no or low stress) or zeaxanthin (high stress) [20]. In this structure, the carotenoids are in van der Waals contact with the chlorophylls [9]. This is essential as carotenoids in LHCII act as accessory light-harvesting pigments

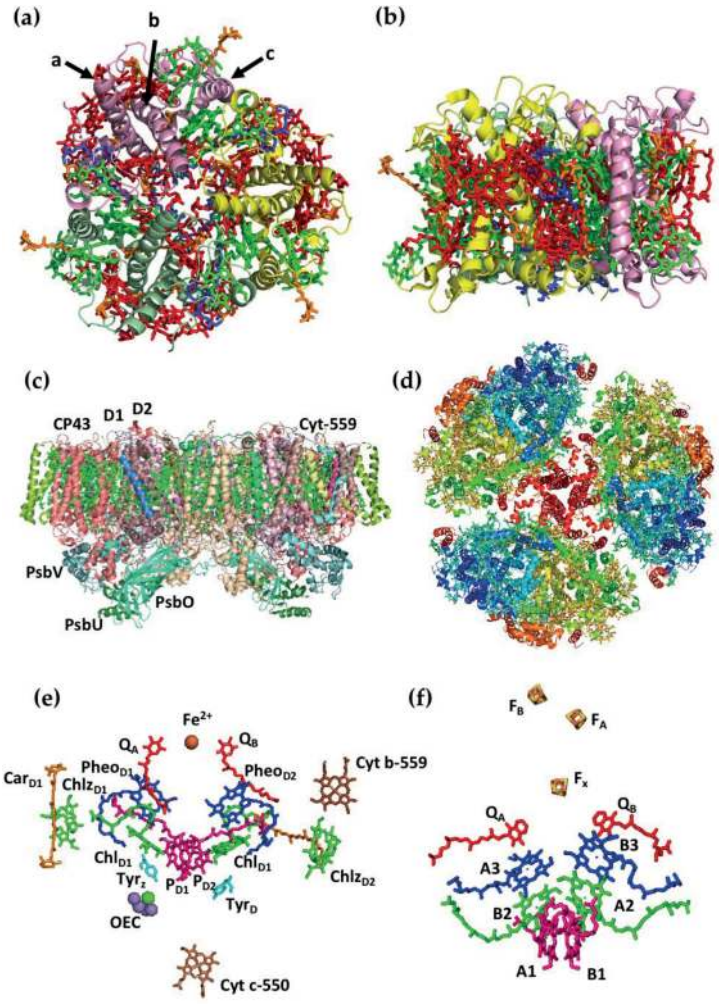

Figure 4. (a) A view looking down on the top of trimeric complex of LHCII structure from spinach. Each monomer is colored magenta, yellow and pale green. The three-transmembrane helices (a, b and c) present in a monomer are labeled and are easily visible. Chl *a* molecules are in red, Chl *b* colored green and carotenoids colored orange. (b) Side-view of LHCII structure shows chlorophyll and carotenoid molecules are packed densely and close to each other (within van der Waals contact), enabling the crucial photo-protective role of these molecules to function by quenching triplet chlorophyll excited states. (c) Structure of PSII from *Thermosynechococcus elongatus* [28], a side-view representation of the overall dimer perpendicular normal with the pseudo-twofold symmetry axis. (e) PSII core reaction center is shown; component co-factors of the electron transport chain viewed along the membrane plane. The two branches are related by the pseudo-twofold symmetry axis. The respective pairs of pigments on the branches are labeled to indicate whether the Mg^{2-} is coordinated by D1, D2. (d) Structure of PSI from *Synechococcus elongatus* [29]; overview of the complete trimer looking along the membrane normal from the stromal side with each polypeptide of the trimer colored differently and chlorophyll molecules given in green. The two main proteins that comprise a monomer are PsaA (yellow) and PsaB (magenta). The electron transport chains are in the center of each monomer. (f) PSI core reaction center component co-factors of the electron transport chain are viewed along the membrane plane. The two branches are related by the pseudo-twofold symmetry axis. The representative pair of chlorophyll molecules on the branches are labeled A or B indicating whether the Mg^{2+} is coordinated by PsaA or PsaB. The iron–sulfur center of F_x involves residues from both PsaA and PsaB, while F_A and F_B are located in an extrinsic subunit called PsaC.

and photoprotectors. The accessory light-harvesting function represents singlet-singlet energy transfer from the carotenoid to the chlorophylls. Since the singlet excited state lifetime of the carotenoid is quite short, approximately 200 fs, the carotenoid must be in close distance to a chlorophyll molecule if the energy transfer is to be efficient. Photoprotection function represents the quenching of triplet excited state of chlorophylls and so preventing the formation of singlet oxygen. This triplet-triplet exchange reaction also requires the carotenoid to be in close contact with the chlorophylls. Regarding CP29, it binds 3 carotenoids and 13 chlorophyll molecules [18]. The position of some chlorophyll binding sites in CP29 differs from LHCII.

The current high-resolution crystal structure of PS II and PSI core complexes is limited to that from cyanobacteria and from pea, respectively [21, 22]. The core of PSII is a multi-subunit complex. Most of the chromophores involve light harvesting as well as electron transfer reaction and are bound to four main subunits, that is, D1, D2, CP43 and CP47. When the core of PSII and PSI reaction center structures is compared, the arrangement of the pigments and other electron transfer co-factors is also very similar (**Figure 4c** and **d**). Here, first we look at the PSII core reaction center. The core of reaction center of PSII is made from two major polypeptides called D1 and D2; each contains five membrane-spanning α-helices. These two helices clasp each other like two cupped hands holding on to each other. The redox cofactors are arranged into two arms that lie on either side of the point where the two groups of helices interact. This arrangement of the helices and the cofactors introduces a pseudo two-fold symmetry axes that runs through the center of reaction center normal to the plane of the membrane. In **Figure 4e**, it is seen that the electron transport pathway in PSII begins with a pair of chlorophyll molecules called P680 (P_{D1} and P_{D2}). Then each arm contains, in order, one monomeric chlorophyll molecule, one pheophytin (a chlorophyll derivative) and one plastoquinone molecule. Here, only the D1 arm is active in electron transport. Upon excitation P680 becomes oxidized and one electron is injected out and passes down the active branch to the quinone Q_A. P680 is re-reduced by electron transfer from a special tyrosine residue called Z (Tyr_z). A second turnover of P680 delivers a second electron to the plastoquinone and the secondary quinone Q_B is now reduced to Q_BH_2. The hole on Tyr_z is filled by electron transfer from the manganese cluster, the oxygen evolving complex. Every four turnovers of P680 stores four positive charges in the manganese cluster that are then used to oxidize water and evolve oxygen. While in CP43 and CP47, there are a total of 49 Chl *a* molecules that are bound and that function as internal antenna and allow excitation energy transfer from the peripheral antenna system to the reaction center.

Unlike PSII, in PS I, the same single polypeptides contain both antenna complexes (Lhca) and the reaction center core. The 3.3 Å resolution crystal structure of PSI from pea showed that plant PSI binds at least 173 Chl *a* and *b* molecules [22]. At this resolution of the crystal structure, it is not possible to identify the Chl species, but biochemical analysis of purified PSI indicated that it has a Chl *a*/*b* ratio in a range of 8.2–9.7 [23, 24]. A large number of Chl *a* and *b* molecules are bound to the Lhca protein, only about 100 Chl *a* are bound in the core complex, and the rest of Chl *a* and *b* are between these moieties. The latter represent the so-called "linker" chlorophylls which are located between Lhca monomers and "gap" chlorophylls (between Lhca and PSI core). The linker chlorophyll molecules probably play an important role in excitation energy transfer between Lhca antennas and from Lhca to the PSI core [20, 25, 26]. Based on biochemical analysis, PSI was reported to bind approximately

33/34 carotenoids, that is, about 12 carotenoid molecules are bound to Lhca, at the interface between Lhca and the core complex, and about 22 β-carotene are bound to the core [20, 23, 26]. Based on these biochemical analysis, it can be estimated that PSI-LHCII supercomplex contains about 215 chlorophyll and 45/46 carotenoid molecules.

The core complex of PSI is composed of smaller number of subunits (15 subunit) than PSII. The large PsaA and PsaB subunit, which contain 11 trans-membrane helices each, forms a heterodimer that binds ~80 Chl *a* and ~20 β-carotene as cofactors for light harvesting as well as 6 Chl *a*, 2 phylloquinones and a 4Fe-4S cluster as cofactors for electron transfer reaction, with the exception of terminal electron acceptors (Fe-S clusters F_A and F_B) which are bound to the PsaC subunit [25]. At closer look (**Figure 4f**), the redox co-factors in the core reaction center are arranged into two arms that are located on either side of the region where two groups of helices interact with each other. Two chlorophylls form P700 and then each arm contains two monomeric chlorophyll molecules (the second one being in the equivalent position to the pheophytin present in photosystem II) followed by one quinone molecule. When P700 is oxidized, both arms of the electron transport pathway are able to work as it was reported that the electron can pass either down the B-branch or the A-branch [27].

4. Chromatographic isolation and identification

Chlorophyll and carotenoid can be isolated as free pigments, detached from the pigment-protein complexes, by organic solvent extraction. Important aspects such as the choice of organic solvents, light exposure and working temperature should be considered while isolating pigments. Based on the structure, chlorophyll is characterized with polar macrocycle ring with non-polar hydrocarbon tail. The structural difference between Chl *b* and Chl *a* is by having an aldehyde group in place of the methyl group at the macrocycle side group. This change is effecting the polarity of Chl *b* to be more polar in comparison to Chl *a*. In the case of carotenoid, structural difference can be seen from the number of conjugated double bonds and the presence of oxygen atoms. Considering these characteristics, mixtures of miscible polar and semi/non-polar solvents are used commonly to extract plant pigments. The mixture of solvent has double functions, that is, penetrating tissues/matrixes and extracting pigments from their lipophilic surrounding. During extraction, exposure of light should be avoided to reduce photodamage of the pigments. Temperature is also important. It is recommended to conduct extraction at lower temperatures, for example, on ice or using liquid nitrogen, to minimize activity of enzyme (e.g. chlorophyllase) that will catalyze breakdown. Antioxidant agent can be also added during extraction to avoid any unwanted oxidation.

After successful isolation, liquid chromatography has been widely used as an effective technique to separate individual type of pigments and for further purification. In this technique, the pigment separation is based on the polarity which depends on the interaction of pigment with the stationary and mobile phases. Elution method either normal phase or reversed phase is chosen according to the type of pigment to be separated. In addition, the choice of liquid chromatographic methods, namely thin layer chromatography (TLC), column chromatography (CC) and high-pressure liquid chromatography (HPLC), is referred to the speed,

resolution and quantity of sample [30]. Currently, ultra-fast liquid chromatography (UFLC), a recent development of HPLC, has been used as a standard for liquid chromatography to achieve high-resolution data with low time consumption [31]. Purification with non-chromatographic method has also been developed, that is, purification method using dioxane has been effective to separate chlorophyll from most of the carotenoids and some lipids [32].

Various types of column absorbents used for chromatographic separation of plant pigments have been well reviewed [30]. Here, we used a silica C30 column attached to UFLC analytic to achieve well separation of carotenoids from *Pleomele angustifolia* leaf using elution gradient program with mixture of water, methanol and methyl tert-butyl ether to separate, at least, 7 dominant pigments within 25 min. (**Figure 5**). The detailed identification of pigments, based on the chromatographic, spectrophotometric and mass properties, is summarized in **Table 1**. Chlorophyll a and chlorophyll b, α- and β-carotenes and violaxanthin are found to be the main chlorophylls and carotenoids, respectively, while the presence of lutein and zeaxanthin in this chloroplast is in low amount.

Larger-scale separation of Chl *a* and *b* can be achieved by CC using Sepharose CL-6B as the stationary phase and a mixture of 2-propanol (IPA) and hexane as the mobile phase. Chl *a* could be eluted using 1.5% IPA in hexane and Chl *b* with 10% IPA in hexane [33]. To achieve a pure, free carotenoid, saponification step is sometimes necessary to eliminate contamination of lipids and chlorophylls. Moreover, carotenoid ester can be hydrolyzed to produce parent carotenoid by using this method [34]. CC is usually used for carotenoid isolation in high quantity of pigment extract. Generally, the purpose of CC is to separate mixtures into carotenoid fractions which are either having high purity to be processed to crystallization or low purity to be extensively separated with further chromatography, that is, HPLC [35].

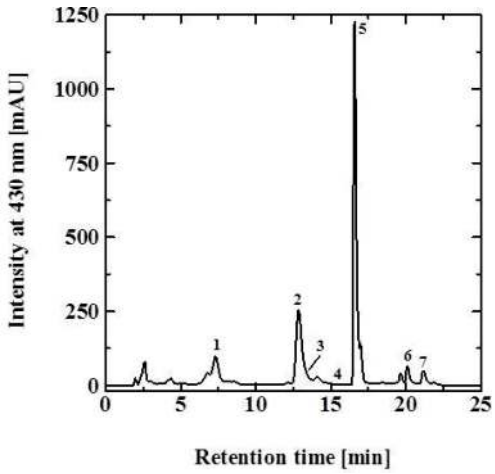

Figure 5. UFLC chromatogram of pigment extract from chloroplast of *Pleomele angustifolia* detected at 430 nm. The UFLC separation condition was as follows: Pigment separation was performed using UFLC equipped with PDA (Shimadzu) on C30 column (150 × 4.6 mm I.D; YMC) with a gradient elution program of water, methanol and methyl tert-butyl ether (MTBE) at the flow rate of 1 mL/min at 30°C.

Peak No	t_R [min]	λ_{maxs} [nm]				Molecular ion	Fragment ions [*m*/*z*]	Identification
		HPLC eluent	Hexane	Ethanol	Acetone	species [*m*/*z*]		
1	7.3	412,436,464	—	—	—	—	—	Violaxanthin
2	12.8	470,601,650	451,595,642	465,601,649	458,596,646	907.7 $[M]^+$	881.7 $[M - COH]^+$	Chlorophyll *b*
							855.7 $[M - COH - Mg]^+$	
3	13.4	422,445,472	422,444,473	–,446,474	–,448,476	568.4 $[M]^+$	551.4 $[M - OH]^+$	Lutein
							476.4 $[M - 92]^+$	
							430.3 $[M - 138]^+$	
4	15.3	–,451,477	425,449,478	425,451, 478	428,454,481	568.6 [M]+	476.4 $[M - 92]^+$	Zeaxanthin
5	16.6	431,618,664	427,613,661	430,616,664	431,617,662	893.5 $[M]^+$	871.5 $[M - Mg]^+$	Chlorophyll *a*
							615.2 $[M - phytyl]^+$	
6	20.1	421,446,473	421,445,474	421,446,476	422,445,473	536.6 $[M]^+$	445.4 $[M + H - 92]^+$	*α*-carotene
7	21.2	–,452,478	–,451,479	–,453,480	–,454,482	536.6 $[M]^+$	444.5 $[M - 92]^+$	*β*-carotene

Table 1. Chromatographic, spectrophotometric and mass properties of pigments separated from the chloroplast of *Pleomele angustifolia*.

http://dx.doi.org/10.5772/intechopen.75672

Silica and alumina are frequently used as the absorbent in the CC with the normal phase elution to separate the distinct carotenoids; however, it is not easy to use this method to separate carotenoid isomers, that is, geometrical isomers, diastereoisomers, and so on. In this case HPLC/UFLC can be used to overcome the difficulty in the separation of carotenoids by CC. Turcsi et al. (2016) revealed that the polar carotenoids including optical isomers, and region and geometrical isomers as well as non-polar carotenes, could be well separated by HPLC on C18 and C30 columns, respectively [36]. High purity of isolated pigment can be achieved by HPLC and crystallization processes. UFLC analysis of the purified zeaxanthin shows that this carotenoid had a high purity of around 99.3% (**Figure 2**, left). All purified pigments have purity higher than 95% (**Figure 6**).

Chromatographic, spectrophotometric and mass properties of pigment are minimum requirements for pigment identification [35]. These properties for all purified pigments are shown in the **Table 1**. In **Figure 7** (right), absorption spectra of the purified chlorophyll a and the purified β-carotene in acetone have the same maximum absorption wavelength (λ_{max}) and other spectral properties, such as the fine structure and spectrum shape, compared to these pigments in the references [37, 38]. Absorption spectrum of chlorophyll a in acetone shows typical Soret (431 nm), Qx (617 nm) and Q_y (662 nm) bands, while two well-defined peaks in the absorption spectrum of β-carotene are found at 454 and 482 nm. This pigment analysis based on the results of spectrophotometer UV–Vis could support the advance pigment analysis using HPLC/UFLC equipped with photodiode array detection and coupled with the mass spectrometry. The LCMS technique has provided a power tool for pigment identification [39, 40]. Tentative identification for zeaxanthin peak separated by HPLC/UFLC analysis with PDA revealed that zeaxanthin has similar retention time (t_R), maximum absorption wavelength (λ_{max}) and the shape of absorption spectrum (data not shown) compared to the isolated

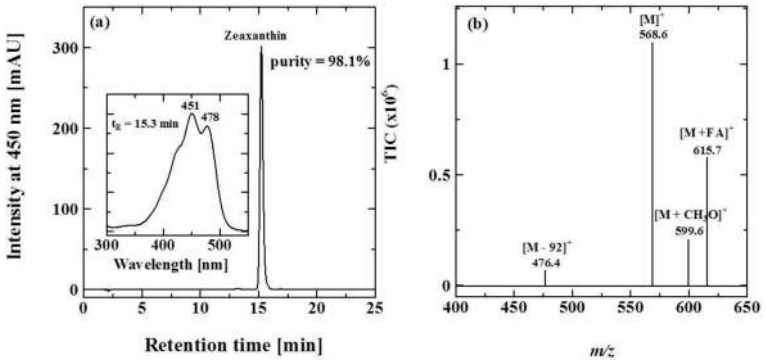

Figure 6. Purification of zeaxanthin: (a) chromatogram detected at 450 nm. Insert figure is UV–Vis spectrum measured by UFLC diode array detector in the eluent and (b) ESI-MS/MS spectrum identification. The conditions of UFLC and ESI-MS/MS analysis were as follows: UFLC analysis of the purified zeaxanthin was performed using UFLC equipped with PDA (Shimadzu) on C30 column (150 × 4.6 mm I.D; YMC) with a gradient elution program of water, methanol and MTBE at the flow rate of 1 mL/min at 30°C. The purified zeaxanthin was directly analyzed to LCMS 8030 (Shimadzu) with an isocratic elution of 0.1% formic acid (FA) in water (10%) and 0.1% FA in methanol (90%) at the flow rate of 0.3 mL/min. MS analysis was operated under the following conditions: (1) heat block temperature = 400°C; (2) desolvation line temperature = 250°C; (3) nebulizing N2 gas flow = 3 L/min; (4) drying N2 gas flow = 15 L/min; (5) interface voltage = 4.5 kV; (6) interface current = 0.1 μA; (7) mass range 400–700 m/z; (8) ionization mode = positive and negative.

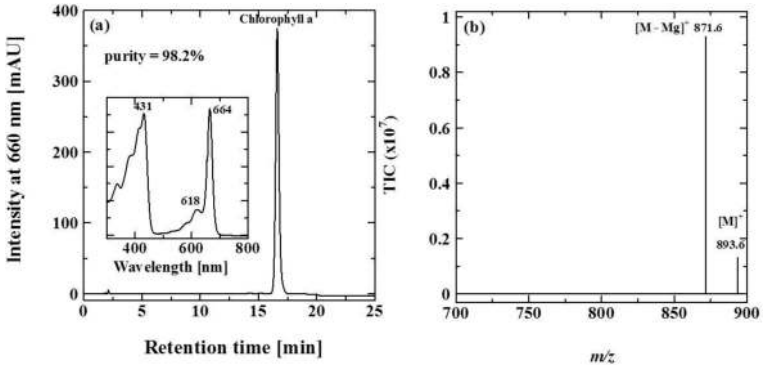

Figure 7. Purification of Chl: (a) chromatogram detected at 660 nm. Insert figure is UV–Vis spectrum measured by UFLC diode array detector in the eluent and (b) ESI-MS/MS spectrum. The condition of UFLC and ESI-MS/MS analysis was as follows: UFLC analysis of the purified chlorophyll a was performed using HPLC equipped with PDA (Shimadzu) on C30 column (150 × 4.6 mm I.D; YMC) with a gradient elution program of water, methanol and MTBE at the flow rate of 1 mL/min at 30°C. The purified chlorophyll a was directly analyzed to LCMS 8030 (Shimadzu) with an isocratic elution of 0.1% formic acid (FA) in water (10%) and 0.1% FA in methanol (90%) at the flow rate of 0.3 mL/min. MS analysis was operated under the following conditions: (1) heat block temperature = 400°C; (2) desolvation line temperature = 250°C; (3) nebulizing N2 gas flow = 3 L/min; (4) drying N2 gas flow = 15 L/min; (5) interface voltage = 4.5 kV; (6) interface current = 0.1 μA; (7) mass range 400–1000 m/z; (8) ionization mode = positive and negative.

zeaxanthin from corn which is a well-known source of zeaxanthin [41]. In addition the mass analysis provides the precursor and fragment ions at the specific *m/z* and characteristic fragmentation pattern for pigment identification. Mass spectrum of Chl *a* indicated the molecular ion $[M]^+$ detected at m/z 893.6 and a fragment ion $[M\text{-}Mg]^+$ at m/z 871.6 related to the loss of magnesium as the central metal of chlorophyll (**Figure 1**). This mass spectrum of Chl *a* agrees with the result that was reported [42].

5. Conclusions

Chlorophyll and carotenoid are chloroplast pigments which are bound non-covalently to protein as pigment-protein complex and play a vital role in photosynthesis. Their functions include light harvesting, energy transfer, photochemical redox reaction, as well as photoprotection. The exact number and stoichiometry of these pigments in higher plants are varied, but their compositions include Chl *a*, Chl *b*, lutein, neoxanthin, violaxanthin, zeaxanthin and β-carotene. Liquid chromatography methods are well developed to separate and purify different types of pigments. Identification and characterization of pigments can be well observed by spectroscopy methods such as UV–Vis absorption, fluorescence and mass spectrometry.

Acknowledgements

Tatas Hardo Panintingjati Brotosudarmo (THPB) acknowledges the competence research grant (No. 120/SP2H/LT/DRPM/IV/2017) from Kemenristekdikti for the financial support.

We also acknowledge Chandra Ayu Siswanti who helped in preparation of chloroplast isolation, pigment isolation and UFLC separation works. We acknowledge Dr. Hendrik Octendy Lintang for supporting fluorescence measurements of photosystem II and I in chloroplast.

Author details

Tatas Hardo Panintingjati Brotosudarmo[1]*, Leenawaty Limantara[2], Rosita Dwi Chandra[1] and Heriyanto[1]

*Address all correspondence to: tatas.brotosudarmo@machung.ac.id

1 Ma Chung Research Center for Photosynthetic Pigments (MRCPP), Chemistry Study Program, Universitas Ma Chung, Malang, Indonesia

2 Universitas Pembangunan Jaya, Banten, Indonesia

References

[1] Porra RJ. Recent progress in porphyrin and chlorophyll biosynthesis. Photochemistry and Photobiology. 1997;**65**:492-516

[2] Adamson HY, Hiller RG, Vesk M. Chloroplast development and synthesis of chlorophyll a and b and chlorophyll protein complexes I and II in the dark in *Tradescantia albiflora* (Kunth). Planta. 1980;**150**:267-274

[3] Lopez-Juez E, Pyke KA. Plastids unleashed: Their development and their integration in plant development. The International Journal of Developmental Biology. 2005;**49**:557-577

[4] Britton G. Biosynthesis of carotenoid. In: Goodwin T, editor. Plant Pigments. San Diego: Academic Press Limited; 1988. pp. 133-279

[5] Rodríguez-Villalón A, Gas E, Rodríguez-Concepción M. Colors in the dark a model for the regulation of carotenoid biosynthesis in etioplasts. Plant Signaling & Behaviour. 2009; **4**:965-967

[6] Scheer H. An overview of chlorophylls and bacteriochlorophylls: biochemistry, biophysics, functions and applications. In: Grimm B, Porra RJ, Rüdiger W, Scheer H, editors. Chlorophylls and Bacteriochlorophylls: Biochemistry, Biophysics, Functions, and Applications. Dordrecht: Springer; 2006. p. 1-26

[7] Gouterman M. Optical spectra and electronic structure and porphyrins and related rings. In: Dolphyn D, editor. The porphyrins. New York: Academic Press; 1978. p. 1-156

[8] Weiss C. Electronic absorption spectra of chlorophylls. In: Dolphyn D, editor. The porphyrins. New York: Academic Press; 1978. p. 211-223

[9] Frank HA, Cogdell RJ. The photochemistry and function of carotenoids in photosynthesis. In: Young A, Britton G, editors. London: Chapman & Hall; 1993. p. 252-326

[10] Nagae H, Kuki M, Cogdell RJ, Koyama Y. Shift of the $^1A_g^- \rightarrow {}^1B_u^+$ electronic absorption of carotenoids in nonpolar and polar solvents. The Journal of Chemical Physics 1994; **101**:6750-6765

[11] Croce R, Müller MG, Bassi R, Holzwarth AR. Carotenoid-to-chlorophyll energy transfer in recombinant major light-harvesting complex (LHCII) of higher plants. I. Femtosecond transient absorption measurements. Biophysical Journal. 2001;**80**:901-915

[12] Holt NE, Kennis JTM, Dall'Osto L, Bassi R, Fleming GR. Carotenoid to chlorophyll energy transfer in light harvesting complex II from *Arabidopsis thaliana* probed by femtosecond fluorescence upconversion. Chemical Physics Letters. 2003;**379**:305-313

[13] Ramel F, Birtic S, Cuiné S, Triantaphylidès C, Ravanat JL, Havaux M. Chemical quenching of singlet oxygen by carotenoids in plants. Plant Physiology. 2012;**158**:1267-1278

[14] Ramel F, Birtic S, Ginies C, Soubigou-Taconnat L, Triantaphylidès C, Havaux M. Carotenoid oxidation products are stress signals that mediate gene responses to singlet oxygen in plants. Proceedings of the National Academy of Sciences of the United States of America. 2012;**109**:5535-5540

[15] Jahns P, Holzwart AR. The role of the xanthophyll cycle and of lutein in photoprotection of photosystem II. Biochimica et Biophysica Acta. 1817;**2012**:182-193

[16] Gracía-Plazaola JI, Esteban R, Fernández-Marín KI, Porcar-Castell A. Thermal energy dissipation and xanthophyll cycles beyond the *Arabidopsis* model. Photosynthesis Research. 2012;**113**:89-103

[17] Liu Z, Yan H, Wang K, Kuang T, Zhang J, Gui L, An X, Chang W. Crystal structure of spinach major light-harvesting complex at 2.72Å resolution. Nature. 2014;**428**:287-292

[18] Pan X, Li M, Wan T, Wang L, Jia C, Hou Z, Zhao X, Zhang J, Chang W. Structural insights into energy regulation of light-harvesting complex CP29 from spinach. Nature Structural and Molecular Biology. 2011;**18**:309-315

[19] Standfuss J, Terwisscha van Scheltinga AC, Lamborghini M, Kühl-Brandt W. Mechanisms of photogrotection and nonphotochemical quenching in pea light-harvesting complex at 2.5Å. EMBO Journal. 2005;**24**:919-928

[20] Ruban AV, Lee PJ, Wentworth M, Young AJ, Horton P. Determination of the stoichiometry and strength of binding of xanthophylls to the photosystem II light harvesting complexes. Journal of Biological Chemistry. 1999;**274**:10458-10465

[21] Umena Y, Kawakami K, Shen JR, Kamiya N. Crystal structure of oxygen-evolving photosystem II at a resolution of 1.9Å. Nature. 2011;**473**:55-60

[22] Amunts A, Toporik H, Horovikova A, Nelson N. Structure determination and improved model of plant photosystem I. The Journal of Biological Chemistry. 2010;**285**:3478-3486

[23] Galka P, Santabarbara S, Khuong TT, Degand H, Morsome P, Jennings RC, Boekema EJ, Caffarri S. Functional analysis of the plant photosystem I-light-harvesting complex II supercomplex reveal that light-harvesting complex II loosely bound to photosystem II is very efficient antenna for photosystem I in state II. Plant Cell. 2012;**24**:2963-2978

[24] Wientjes E, Oostergetel GT, Jansson S, Boekema EJ, Croce R. The role of Lhca complees in the supramolecular organization of higher plant photosystem I. Journal of Biological Chemistry. 2009;**284**:7803-7810

[25] Ben-Shem A, Frolow F, Nelson N. Crystal structure of plant photosystem I. Nature. 2003;**426**:630-635

[26] Ballottari M, Govoni C, Caffarri S, Morosinotto T. Stoichiometry of LHCI antenna polypeptides and characterization of gap and linker pigments in higher plants photosystem I. European Journal of Biochemistry. 2004;**271**:4659-4665

[27] Santabarbara S, Kuprov I, Fairclough WV, Purton S, Hore PJ, Heathcote P, Evans MCW. Bidirectional electron transfer in photosystem I: Determination of two distances between P_{700}^{+} and A_1^{-} in spin-correlated radical pairs. Biochemistry. 2005;**33**(6):2119-2128

[28] Loll B, Kern J, Saenger W, Zouni A, Biesiadka J. Toward complete cofactor arrangement in 3.0 Å resolution structure of photosystem II. Nature. 2005;**438**:1040-1044

[29] Jordan P, Fromme P, Witt HT, Klukas O, Saenger W, Krauß N. Three-dimensional structure of cyanobacterial photosystem I at 2.5 Å resolution. Nature. 2001;**x411**:909-917

[30] Shioi Y. Large scale chlorophyll preparation using simple open-column chromatographic methods. In: Grimm B, Porra RJ, Rüdiger W, Scheer H, editors. Chlorophylls and Bacteriochlorophylls: Biochemistry, Biophysics, Functions, and Applications. Dordrecht: Springer; 2006. p. 122-131

[31] Yan B, Zhao J, Brown JS, Blackwell J, Carr PW. High-temperature ultrafast liquid chromatography. Analytical Chemistry. 2000;**72**:1253-1262

[32] Iriyama K, Ogura N, Takamiya A. A simple method for extraction and partial purification of chlorophyll from plant material using dioxane. Journal of Biochemistry. 1974; **76**:901-904

[33] Karcz D, Borón B, Matwijczuk A, Furso J, Starón RA, Fiedor L. Lessons from chlorophylls: Modifications of porphyrinoids towards optimized solar energy conversion. Molecules. 2014;**19**:15938-15954

[34] Wang T, Han J, Tian Y, Zhang D, Wang Y, Wu Y, Ni L. Combined process of reaction, extraction and purification of lutein in marigold flower by isopropanol-KOH aqueous two-phase system. Separation Science and Technology. 2016;**51**:1490-1498

[35] Britton G, Liaaen-Jensen S, Pfander H. Carotenoid. Volume 1A: Isolation and Analysis. Basel: Birkhauser Verlag; 1995. p. 328

[36] Turcsi E, Nagy V, Deli J. Study on the evaluation of carotenoid on endcapped C_{18} and C_{30} reverse silica stationary phases – A review of the database. Journal of Food Composition and Analysis. 2016;**47**:101-112

[37] Jeffrey SW, Mantoura RFC, Wright SW. Phytoplankton Pigments in Oceanography: Guidelines to Modern Methods. Paris: UNESCO Publishing; 1995

[38] Britton G, Liaaen-Jensen S, Pfander H. Carotenoid Handbook. Basel: Springer; 2004

[39] van Breemen RB. Electrospray liquid chromatography-mass spectrometry of carotenoid. Analytical Chemistry, 1995;67(13):2004-2009

[40] Rivera SM, Christou P, Canela-Garayoa R. Identification of carotenoids using mass spectrometry. Mass Spectrometry Reviews. 2014;**33**:353-372

[41] Scott CE, Eldridge AL. Comparison of carotenoid content in fresh, frozen and canned corn. Journal of Food Composition and Analysis. 2005;**18**:551-559

[42] Heriyanto JAD, Shioi Y, Limantara L, Brotosudarmo THP. Analysis of pigment composition of brown seaweeds collected from Panjang Island, Central Java, Indonesia. The Philippine Journal of Science. 2017;**146**:323-330